Arbitrary-Shaped Graphene-Based Planar Sandwich Supercapacitors on One Substrate with Enhanced Flexibility and Integration

Shuanghao Zheng,[†,§,‡] Xingyan Tang,[‖] Zhong-Shuai Wu,*[,†] Yuan-Zhi Tan,[‖] Sen Wang,[†,‡] Chenglin Sun,[†] Hui-Ming Cheng,[#,⊥] and Xinhe Bao[†,§]

[†]Dalian National Laboratory for Clean Energy, Dalian Institute of Chemical Physics and [§]State Key Laboratory of Catalysis, Dalian Institute of Chemical Physics, Chinese Academy of Sciences, 457 Zhongshan Road, Dalian 116023, China

[‖]State Key Laboratory for Physical Chemistry of Solid Surfaces and Department of Chemistry, College of Chemistry and Chemical Engineering, Xiamen University, 422 Siming South Road, Xiamen 361005, China

[‡]University of Chinese Academy of Sciences, 19 A Yuquan Rd, Shijingshan District, Beijing 100049, China

[#]Shenyang National Laboratory for Materials Science, Institute of Metal Research, Chinese Academy of Sciences, 72 Wenhua Road, Shenyang 110016, P. R. China

[⊥]Tsinghua-Berkeley Shenzhen Institute (TBSI), Tsinghua University, 1001 Xueyuan Road, Shenzhen 518055, P. R. China

Ⓢ Supporting Information

ABSTRACT: The emerging smart power source-unitized electronics represent an utmost innovative paradigm requiring dramatic alteration from materials to device assembly and integration. However, traditional power sources with huge bottlenecks on the design and performance cannot keep pace with the revolutionized progress of shape-confirmable integrated circuits. Here, we demonstrate a versatile printable technology to fabricate arbitrary-shaped, printable graphene-based planar sandwich supercapacitors based on the layer-structured film of electrochemically exfoliated graphene as two electrodes and nanosized graphene oxide (lateral size of 100 nm) as a separator on one substrate. These monolithic planar supercapacitors not only possess arbitrary shapes, *e.g.*, rectangle, hollow-square, "A" letter, "1" and "2" numbers, circle, and junction-wire shape, but also exhibit outstanding performance ($\sim$280 F cm^{-3}), excellent flexibility (no capacitance degradation under different bending states), and applicable scalability, which are far beyond those achieved by conventional technologies. More notably, such planar supercapacitors with superior integration can be readily interconnected in parallel and series, without use of metal interconnects and contacts, to modulate the output current and voltage of modular power sources for designable integrated circuits in various shapes and sizes.

KEYWORDS: graphene, planar supercapacitors, arbitrary shape, printable, flexible, integration

The rapid development of emerging smart power source-integrated electronics with multiple functionalities of superthinness, flexibility, lightweight, and unusual shape diversity has ultimately accelerated the never-ceasing pursuit of innovative, intelligent, and fully integrated energy storage systems, which can be indispensably compatible with these electronics.[1−4] However, the currently available energy storage systems, *e.g.*, lithium-ion batteries and supercapacitors with fixed shapes (*e.g.*, cylindrical, pouch types), large size, bulk volume, and heavy weight, have been manufactured by stacking and packaging cell components (*e.g.*, two electrodes, separator, current collectors), followed by injection of liquid electrolytes, which cannot definitely fulfill the stringent requirements for the

revolutionized flexible electronics.[5−8] Furthermore, the traditional power sources with huge limitations on the design and performance, *e.g.*, the leakage of liquid electrolytes, use of polymer binder, additive, and thick separator, along with two pieces of flexible substrates (*e.g.*, plastic substrate, textile), cannot keep pace with the progress of shape-tailored, flexible, smart integrated circuits.[9,10]

To overcome these limitations, enormous efforts have been devoted to developing flexible and smart energy storage
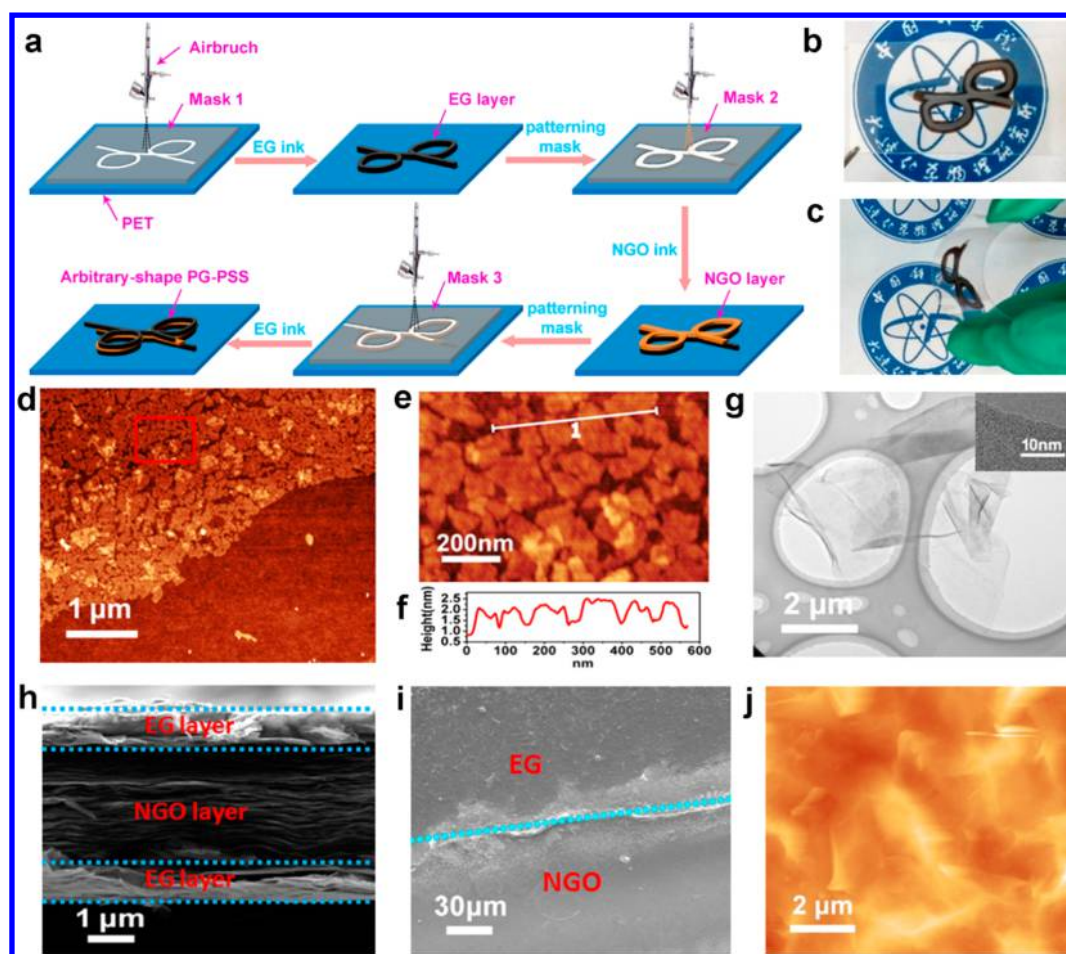
Figure 1. Architecture design, fabrication, and characterization of arbitrary-shaped PG-PSSs. (a) Schematic of the fabrication of arbitrary-shaped PG-PSSs (*e.g.*, junction-wire-shaped) made up of an EG/NGO/EG layer-structured film on a single PET substrate by a printable technique with assistance of alternating customized masks. (b,c) Photographs of the junction-wire-shaped PG-PSSs with (b) flat and (c) bending states. The use of the logo is permitted from Dalian Institute of Chemical Physics, Chinese Academy of Sciences. (d) Low-magnification and (e) high-magnification AFM images and (f) height profile of NGO sheets on a silicon wafer, showing an average lateral size of ~100 nm and uniform thickness of ~1 nm. (g) TEM image of a single-layer EG nanosheet. Inset shows a monolayer EG. (h) Cross-section SEM image of an EG/NGO/EG layer-structured film, showing alternating stacked structures of EG and NGO layers. (i) Top-view SEM image of the stacked edge between the top EG layer and the middle NGO layer in an EG/NGO/EG film. (j) AFM height image of an EG/NGO/EG layer-structured film on a silicon wafer, showing the low average surface roughness of the film with a R_a (roughness average) of ~90 nm.

devices, *e.g.*, supercapacitors,[11−13] with good scalability, flexibility, performance, or shape diversity through rational fabrication of nanostructured electrode materials (such as carbon nanotubes,[14] graphene,[15−19] MXene,[20−23] MoS$_2$[24]), innovation of thin-film scalable fabrication technologies (*e.g.*, spray printing,[25] inkjet printing,[26] 3D printing,[27] and roll-to-roll printing[28]), exploitation of solid-state electrolytes and separators (such as polymer,[29] inorganic ceramics[30]), development of current collectors (*e.g.*, textiles,[31] 3D current collectors,[32,33] and nanoporous gold[34]), use of flexible substrates (such as polyethylene terephthalate (PET),[35] paper,[36] cellulose fibers[37,38]), and creation of device architectures (such as fiber,[39,40] foldable,[41] stretchable[42,43]). So far, most reported energy storage devices with a sandwich-like stacked geometry are substantially dependent on the conventional device assembly, lacking of versatility and integration in form factors, which is a key area but still significantly under-developed.

Recently, a class of planar energy storage devices, *e.g.*, graphene-based planar supercapacitors,[44,45] consisting of interdigital electrodes produced on one single substrate, have spurred great attention since they hold great promise as a

disruptive technology enabling the superior flexibility and miniaturization of electronics for on-chip uses.[46−48] Planar interdigital geometry is of great importance to all device components, including two electrodes, separator, electrolyte, and current collectors, integrated on the same substrate.[12,44,49,50] In such planar geometry, the positive and negative electrodes on the same plane are generally separated by an empty interspace to avoid short circuit.[51,52] One major disadvantage is that the positive electrode and negative electrode cannot absolutely intersect each other to build arbitrary-shaped planar supercapacitors.[53] In addition, the state-of-the-art reported flexible sandwich supercapacitors with a stacked geometry are generally assembled in nonplanar dimension, based on two substrates (*e.g.*, PET, cloth) for supporting thin-film electrodes.[19,54−57] Despite significant progress of planar interdigital supercapacitors and flexible sandwich supercapacitors, the designed construction of arbitrary-shaped planar sandwich supercapacitors on one substrate has not been yet achieved.

Herein, we demonstrate the scalable fabrication of arbitrary-shaped printable graphene-based planar sandwich super-
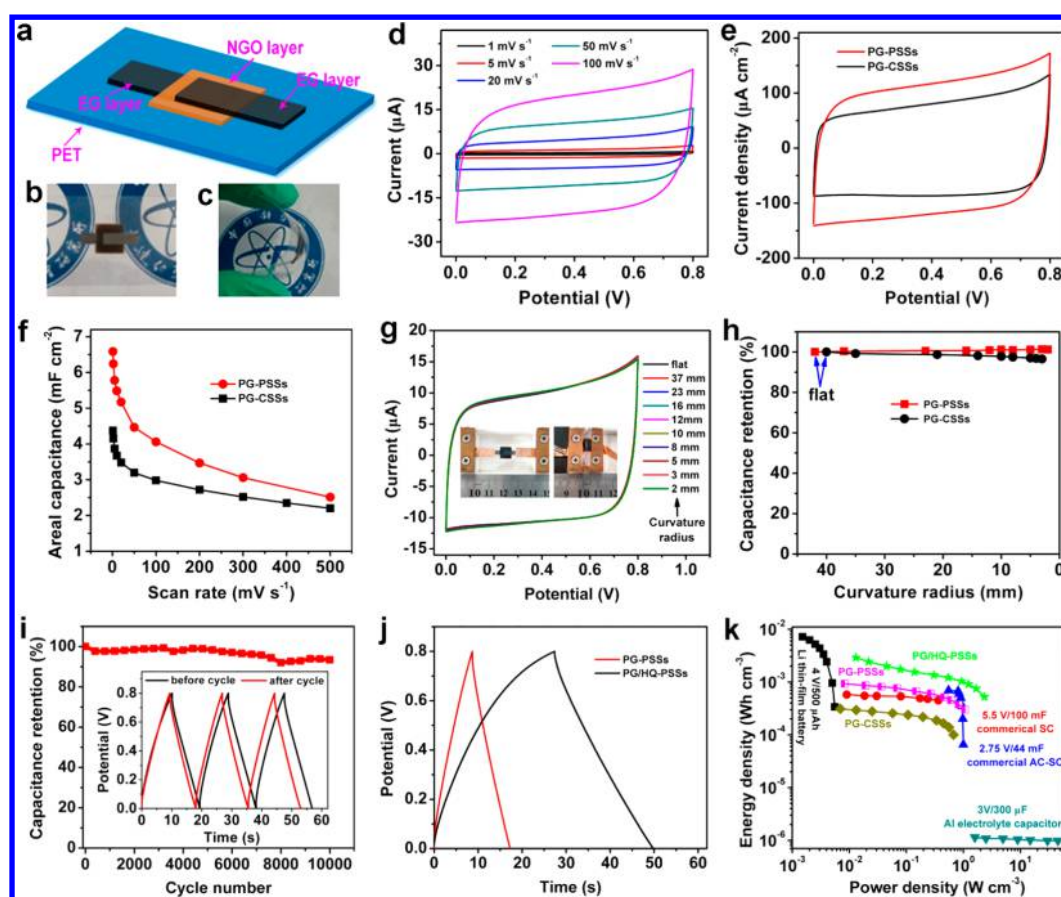
Figure 2. Electrochemical characterization and superiority of rectangle-shaped PG-PSSs. (a) Schematic of a rectangle-shaped PG-PSS made up of an EG/NGO/EG layer-structured film on a single PET substrate. (b,c) Optical images of rectangle-shaped PG-PSSs under (b) flat and (c) bending states. The use of the logo is permitted from Dalian Institute of Chemical Physics, Chinese Academy of Sciences. (d) The CVs of the rectangle-shaped PG-PSSs using a H_2SO_4/PVA gel electrolyte, measured at different scan rates from 1 to 100 mVs^{-1}. (e) The CVs of the rectangle-shaped PG-PSSs and PG-CSSs measured at a scan rate of 50 mV s^{-1}. (f) Performance comparison of areal capacitance of PG-PSSs with PG-CSSs. (g) The CV curves of the rectangle-shaped PG-PSSs bent at different states from 42 (almost flat, inset) to 2 mm ($\geq$180°, inset), indicated by a ruler. (h) Capacitance retention as a function of curvature radius. (i) Cycling stability of rectangle-shaped PG-PSSs for 10,000 cycles. Inset: GCD curves of PG-PSSs at a current density of 200 μA cm^{-2}. (j) GCD curves of PG/HQ-PSSs and PG-PSSs measured at a current density of 200 μA cm^{-2}. (k) Ragone plot of PG/HQ-PSSs, PG-PSSs, and PG-CSSs with commercially available energy storage devices.

capacitors (denoted as PG-PSSs) with excellent performance, excellent flexibility, innovative versatility, and superior integration, based on a monolithic layer-structured film of fully printed, electrochemically exfoliated graphene (EG) as two electrodes and nanosized graphene oxide (NGO, lateral size of ~100 nm) as a separator on one single substrate. The PG-PSSs possess designable geometries and multiple functionalities far beyond those attainable by conventional supercapacitor technologies. First of all, the printable technique allows for the simplified mass production of planar sandwich supercapacitors with arbitrary-shape, *e.g.*, rectangle, hollow-square, "A" letter, "1" and "2" numbers, circle, and even complicated junction-wire shape. Second, the diversity of graphene materials provided a platform for constructing monolithic PG-PSSs, showing exceptional areal capacitance of 6.6 mF cm^{-2} and volumetric capacitance of 94 F cm^{-3} that are superior to conventional flexible supercapacitors. Further, volumetric capacitance of ~280 F cm^{-3} can be substantially enhanced when a redox electrolyte (*e.g.*, hydroquinone) was introduced into the film electrodes. Third, the versatile-shaped PG-PSSs exhibited excellent flexibility, very stable performance without capacitance degradation under different bending states, and excellent cycling stability, *e.g.*, 93% of capacitance retention for

rectangle-shaped PG-PSSs after 10,000 cycles. Importantly, the output capacitance of our devices can be easily modulated by covering gel electrolyte on the selected area of the electrode film. In addition, such arbitrary-shaped PG-PSSs can be readily interconnected in parallel and series to produce modular power sources for designable integrated circuits with exceptional shape conformability and high output current and voltage.

RESULTS AND DISCUSSION

Figure 1a conceptually depicts the stepwise manufacturing procedure of arbitrary-shaped PG-PSSs on a flexible PET substrate by a printable technique. To fabricate PG-PSSs, two different graphene nanosheets were chosen, one was high-quality, solution processable electrochemically EG nanosheets ($\leq$3 layers, Figures 1g and S1) with a large lateral size of 10 μm;[58] another was single-layer NGO sheets with a small average lateral size of ~100 nm (Figures 1d–f and S2) and oxygen-enriched groups (C/O ratio of ~2.2, Figure S3). Afterward, the inks of EG (0.1 mg mL^{-1} in isopropanol) and NGO (1.8 mg mL^{-1} in deionized water) were consecutively printed on a flexible PET substrate with assistance of alternating shape-tailored customized masks to form a shape-designable EG/NGO/EG layer-structured film (Figure 1b,c).

Subsequently, a polymer gel electrolyte of H_2SO_4/poly(vinyl alcohol) (H_2SO_4/PVA) was carefully drop-casted onto the surface of the film and solidified for 12 h. Finally, all solid-state PG-PSSs with complex geometries (Figure 1a) were achieved (see details in the Methods section). Notably, this printable technique is a versatile and reliable mass-production method for PG-PSSs capable of shape and functional versatility because it does not require the traditional manufacturing process of electrode (*e.g.*, polymer binder, additive) and complicated device assembly (*e.g.*, liquid-electrolyte injection, mesoporous separator membrane, current collector).[9,35]

Cross-section SEM image of the layer-structured film shows an alternating stacked layer structure of EG/NGO/EG (Figure 1h). Typically, the thicknesses of the top and bottom EG layers and the middle NGO layer are ~700 nm and ~2 μm (Figure 1h), respectively, which act as electrochemically active electrodes with a high electric conductivity of ~50 S cm^{-1} and separator,[59] respectively. Top-view SEM image of the stacked edge of EG and NGO layer reveals continuous uniformity and excellent interfacial adherence of the EG layer and the NGO layer (Figures 1i and S4). The AFM image further confirms a flat morphology with low surface roughness of 90 nm (Figure 1j). It should be emphasized that the NGO sheets for the middle separator layer are superior to common GO nanosheets with large lateral size (Figures S5 and S6) for the performance improvement of PG-PSSs, taking into consideration the average lateral size of ~100 nm, appropriate *d*-spacing of 0.84 nm (Figure S3a), and rich oxygenated groups (Figure S 3d) in NGO sheets, which could efficiently facilitate fast ion migration of H^+ and H_3O^+ between the sandwiched EG layers for considerable capacitance enhancement (Figure S7).[59] Meanwhile, the addition of foreign electrolyte can significantly improve the capacitance of PG-PSSs, compared to PG-PSSs without gel electrolyte (Figure S8).

To elucidate the superiority of planar sandwich geometry for PG-PSSs, we constructed rectangle-shaped PG-PSSs made up of an EG/NGO/EG film, covering a H_2SO_4/PVA gel electrolyte on a single PET substrate (Figure 2a−c). For comparison, we also fabricated classical sandwich supercapacitors (CSSs) comprising of a H_2SO_4/PVA gel electrolyte between two EG film electrodes with the same film thickness printed on two individual PET substrates (denoted as PG-CSSs, Figure S9). Cyclic voltammetry (CV) experiments were conducted at scan rates ranging from 1 to 100 mV s^{-1} (Figure 2d). From the comparison with PG-CSSs, it is validated that PG-PSSs exhibited remarkably enhanced electrochemical performance with a nearly rectangular CV shape and symmetric shape of galvanostatic charge and discharge (GCD) profiles (Figure S10), indicative of the superior double-layer capacitive behavior. The areal and volumetric capacitances of PG-PSSs were calculated to be ~6.6 mF cm^{-2} and ~94 F cm^{-3}, respectively, both of which were much higher than those of PG-CSSs (4.3 mF cm^{-2} and 62 F cm^{-3}) (Figures 2e,f and S11), and other reported carbon-based thin films for supercapacitors (0.4−2 mF cm^{-2}, and 60−100 F cm^{-3}).[60] This anomalous increase of the capacitance is mainly attributed to the synergetic effect of the electric field and the charged NGO sheets with oxygen-rich groups, making the water much more ordered near the confined NGO layers for the improvement of total charge storage.[59] Furthermore, our PG-PSSs exhibited better rate capability than that of PG-CSSs. For instance, ~4.1 mF cm^{-2} and ~58 F cm^{-3} for areal and volumetric capacitances, respectively, remained at 100 mV s^{-1}, which is 62% of the

initial value at 1 mV s^{-1}. By contrast, low values of ~3.0 mF cm^{-2} and ~42 F cm^{-3} were attained for PG-CSSs. It should be pointed out that PG-PSSs using a thicker NGO layer showed lower capacitance (Figure S12). In addition, Nyquist plots of both PG-PSSs and PG-CSSs displayed nearly vertical lines at low frequency, indicative of excellent capacitive behavior (Figure S13a). In a high-frequency region, PG-PSSs showed an equivalent series resistance of 36 Ω cm^{-2}, which was higher than that of PG-CSSs with 34 Ω cm^{-2}. Further, the characteristic frequency of PG-PSSs at the phase angle of −45° was 3.0 Hz, which was slightly lower than that of PG-CSSs (4.1 Hz, Figure S13b). Correspondingly, the time constant of PG-PSSs and PG-CSSs was 333 and 244 ms, respectively. From this comparison, it can be concluded that our PG-PSSs using NGO as a separator scarcely obstruct the free transfer of electrolyte ions, due to the small lateral size (an average size of 100 nm) and large interlayer space of NGO (0.84 nm).

Notably, our flexible PG-PSSs showed excellent mechanical flexibility (Figure 2g,h) and cycling stability (Figure 2i). It can be seen that the CV shapes of PG-PSSs remained completely unchanged under different bending states from the curvature radius of 42 mm (almost flat) to 2 mm (fully bent ≥180°) (Figure S14), compared to PG-CSSs with an apparent capacity degradation of ~5% (Figures 2h and S15−17). Remarkably, neither structural instability between the EG layer and NGO layer nor delamination of both the layer-structured film and the substrate was observed after bending. Furthermore, 93.4% of initial capacitance was maintained after 10,000 times at a current density of 200 μA cm^{-2} (Figure 2i), much better than the PG-CSSs (90.1%, Figure S18). This finding strongly suggests that the PG-PSSs possess enormous superiority over PG-CSSs on two PET substrates for the flexible energy storage devices.

In an attempt to boost the significant capacitance enhancement of PG-PSSs, we also adopted the same approach to fabricate redox molecule-mediated EG films for PSSs (denoted as PG/HQ-PSSs), incorporating a printable hybrid film of EG and highly pseudocapacitive hydroquinone (HQ),[61] instead of the capacitive EG layer, into planar sandwich cells (see details in the Methods section and Figures 2j and S19). It is disclosed that the PG/HQ-PSSs showed substantially enhanced volumetric capacitance of ~280 F cm^{-3} at 1 mV s^{-1}, three times higher than that of PG-PSSs (94 F cm^{-3} at 1 mV s^{-1}), demonstrative of the advantages of this technique.

The Ragone plot in Figure 2k compares the volumetric energy density and power density of our PG-PSSs and PG/HQ-PSSs to PG-CSSs and other commercially available energy-storage devices.[6,53] Remarkably, our PG/HQ-PSSs offered a volumetric energy density of ~2.9 mWh cm^{-3}, which is much higher than those of PG-PSSs (0.98 mWh cm^{-3}) and PG-CSSs (0.35 mWh cm^{-3}), one order of magnitude higher than those of commercially available supercapacitors (2.75 V/44 mF and 5.5 V/100 mF, < 1 mWh cm^{-3}),[6] and well comparable to that of lithium thin-film batteries (10 mWh cm^{-3}).[60] This value (2.9 mWh cm^{-3}) is one of the highest values among the state-of-the-art thin-film supercapacitors reported (Table S1). Moreover, PG-PSSs manifested a maximum power density of ~2.3 W cm^{-3}, which is superior to those of commercially available supercapacitors (2.75 V/44 mF and 5.5 V/100 mF, <1 W cm^{-3})[6] and comparable to that of high-power electrolytic capacitors.[53]
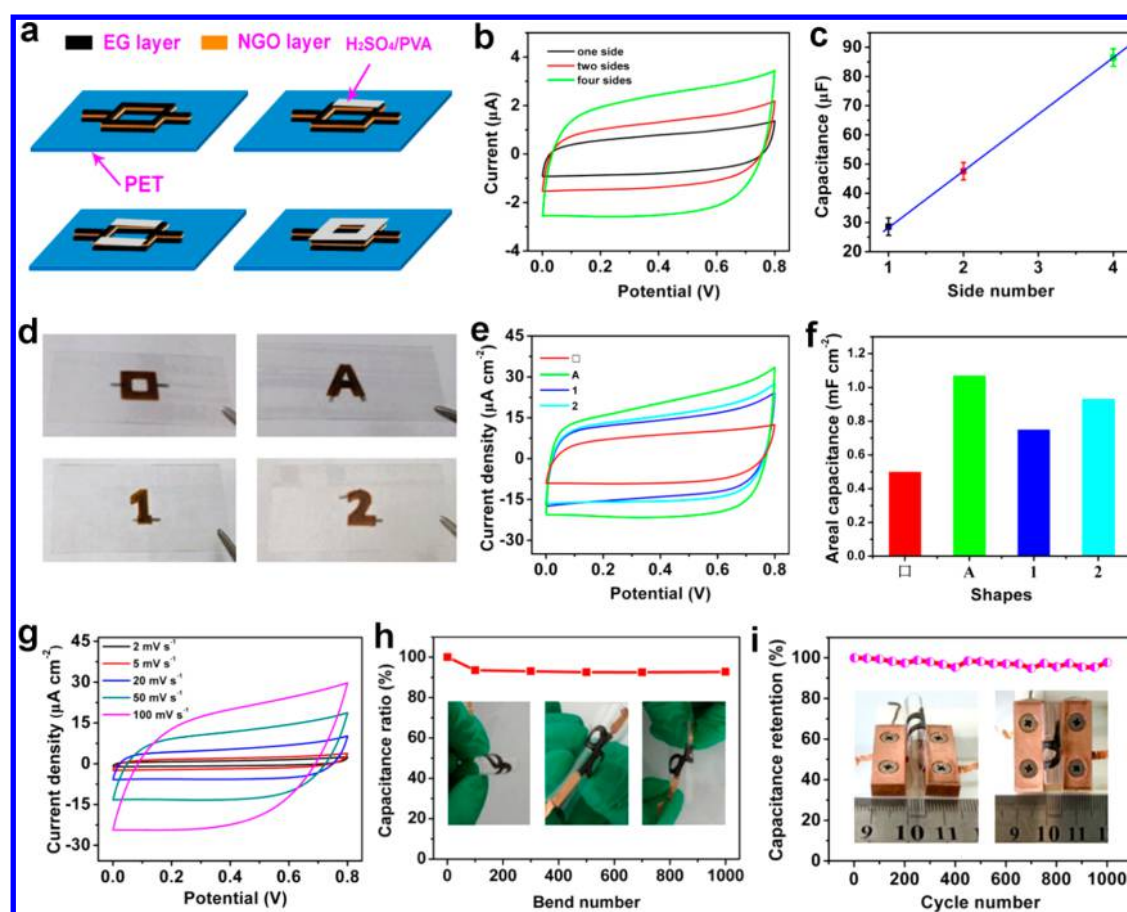
Figure 3. Electrochemical performance and versatility of arbitrary-shaped PG-PSSs. (a) Schematic of hollow square-shaped PG-PSSs (top left) without the addition of H_2SO_4/PVA electrolyte, and the one side (top right), two sides (bottom left), and four sides (bottom right) of hollow square-shaped PG-PSSs covered with the isolated gel electrolyte. (b) The CV curves obtained at 50 mV s^{-1} and (c) capacitance contribution of one side, two sides, and four sides of hollow square-shaped PG-PSSs, showing the stepwise increase of the capacitance. (d) Photographs of different PG-PSSs based on different thick EG layers with a hollow square shape, the letter "A" shape, and the numbers "1" shape and "2" shape, respectively. (e) The CV curves tested at 50 mV s^{-1} and (f) areal capacitance of various arbitrary-shaped PG-PSSs obtained at 2 mV s^{-1}. (g) The CV curves of the junction-wire-shaped PG-PSSs measured at different scan rates. (h) Capacitance retention of the junction-wire-shaped PG-PSSs as a function of the repeated bending number. Insets show three representative bending states. (i) Cycling stability of the junction-wire-shaped PG-PSSs obtained at 100 mV s^{-1} for 1000 cycles under a continuous bending condition. Insets show the top and side view photographs of the bent PG-PSSs.

To satisfy the urgent demands of the future electronics with mechanical flexibility and shape versatility,[62] innovative smart power source systems are highly required to be shape conformable yet mechanically flexible, and also seamlessly integrated with these electronics.[2] In this case, our PG-PSSs hold great promise as a competitive candidate to power next-generation flexible electronics.

To explore the availability of PG-PSSs with unusual shape architecture, we constructed a hollow-square-shaped PG-PSSs based on the printable one-body EG/NGO/EG layer-structured film on a PET substrate with help of a customized mask with the designed shape, as illustrated in Figure 3a. Traditionally, it is well-known that the commonly used electrolyte could completely immerse the two electrodes within each cell, giving rise to the intractable difficulty in the modulation of capacitance from the individual cell.[5] By applying this well-designed configuration, we further validated that the capacitance of one single device could be readily tailored through the elaborated isolation of gel electrolyte on the selected electrode area of the hollow-square layer-structured film. To proof this concept, the isolated H_2SO_4/PVA

electrolyte was exactly coated on one side, two sides, and four sides of hollow square-shaped PG-PSSs, as schematically illustrated in Figure 3a. The CV curves fairly confirm the double increase of current density (Figure 3b) and capacitance contribution (Figure 3c) from one side to two sides and four sides of hollow square-shaped PG-PSSs with the stepwise increase of the electrolyte-covered electrode area in this architecture, suggesting the process superiority of our PG-PSSs as a promising next-generation capacitance-modulated power source.

Except for the above hollow square shape, a series of other arbitrary-shaped PG-PSSs with an "A" letter shape and numbers "1" shape and "2" shape, respectively, were fabricated using the aforementioned printing technique (Figure 3d, see details in the Methods section). Remarkably, all of these versatile-shaped PG-PSSs showed normal CV curves and charge/discharge profiles with a typical EDLC behavior (Figures 3e,f and S20−23), demonstrating both the shape conformability and versatile applicability of our PG-PSSs.

To further highlight the significance of PG-PSSs capable of a more complex shape design, a junction-wire-shaped PG-PSS
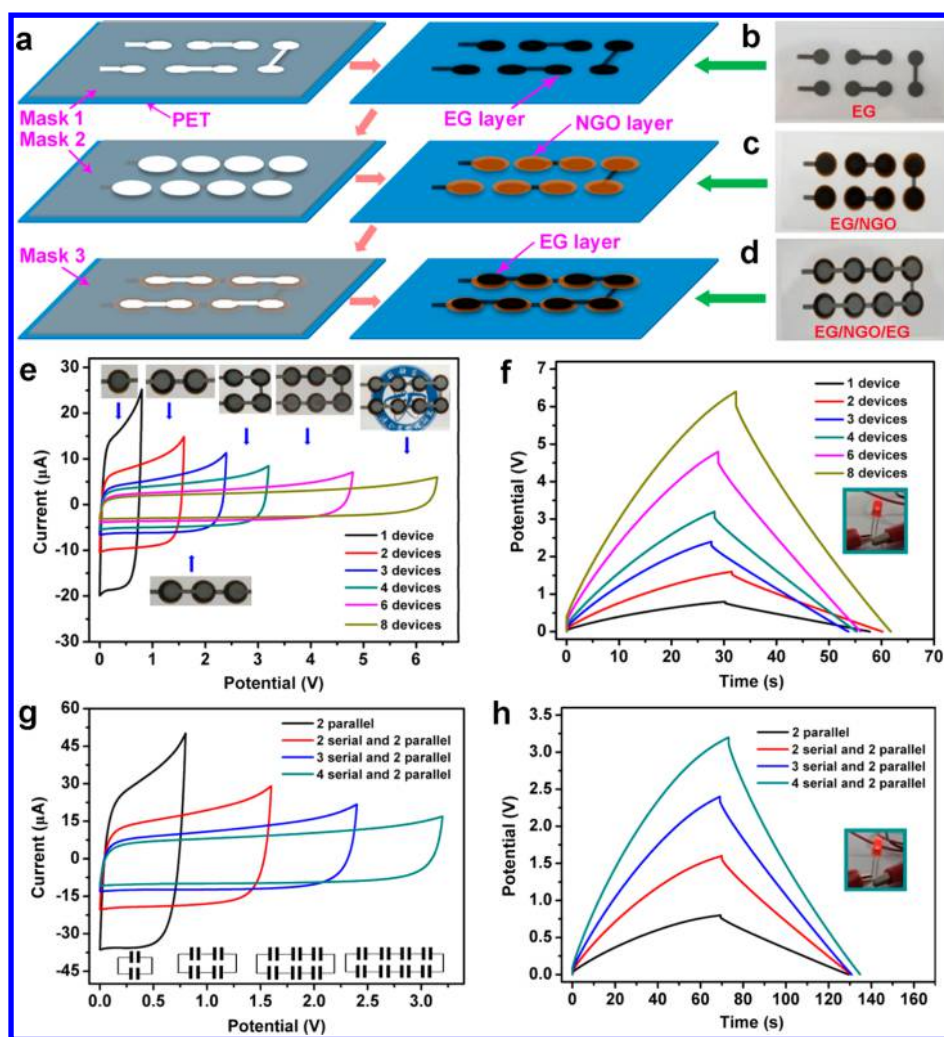
Figure 4. Scalable fabrication and integration of circle-shaped PG-PSSs. (a) Schematic of the simultaneous fabrication and integration of eight circle-shaped PG-PSSs interconnected in series, based on a 300 nm-thick EG layer. (b−d) Photographs of (b) the bottom EG layer, (c) the middle NGO layer, and (d) the top EG layer of eight interconnected circle-shaped PG-PSSs in series. (e) The CV curves obtained at 50 mV s^{-1}, and (f) GCD curves of the serial interconnected pack of PG-PSSs from 1 to 8 devices at current density of 20 μA cm^{-2}. Insets in (e) are the photographs of the integrated PG-PSSs. The inset in (f) is a photograph for powering a LED. (g) CV curves tested at 50 mV s^{-1}, and (h) GCD curves at current density of 20 μA cm^{-2} of the interconnected pack of PG-PSSs in combined connection of 2 parallel and 2 series from 1 to 4 devices. Inset in (h) is a photograph for powering a LED.

was made as an example using this printable technique (Figure 1a). It should be mentioned that such a junction-wire-shaped planar cell cannot be absolutely achieved from the reported energy storage systems, even with a planar geometry, e.g., interdigital, concentric circular, in which a separator gap in the two-dimensional (2D) plane is permanently presented between positive and negative electrodes.[51,53] As for PG-PSSs, a thin NGO film layer as separator sandwiched between two electrodes in the three-dimensional (3D) space could offer the opportunities of planar devices with arbitrary shapes. Figure 3g shows the CV curves of the junction-wire-shaped PG-PSSs measured at different scan rates from 2 to 100 mV s^{-1}. The PG-PSSs presented normal EDLC behavior and an areal capacitance of ∼0.88 mF cm^{-2} (Figures 3g and S24). Furthermore, to evaluate the superior mechanical flexibility of the PG-PSSs, the cells were completely subjected to continuously repeated bending deformation (inserted photographs in Figure 3h) for 1000 times, exhibiting >93.0% of initial capacitance in a flat planar configuration. Remarkably, the PG-PSSs being continuously bent even at a curvature radium of 3

mm still showed no appreciable deterioration after 1000 times (Figure 3i). Special emphasis is given to, during the whole bending process, no observation of any external force-induced shape failure and dimensional disruption, indicative of the superior stability of our PG-PSSs. These results demonstrate the feasibility of our strategy in developing arbitrary-shaped all graphene-based planar supercapacitors with versatile availability and applicability.

Our approach is not limited to the precise manufacture of arbitrary-shaped individual cells, but is scalable for producing interconnected modular power sources, without use of additional metal (oxide)-based interconnects and contacts, which could overcome the design and performance bottlenecks of traditional power sources that cannot satisfy the stringent requirements of integrated circuits with exceptional shape conformability and high output current and voltage. Figure 4a shows a representative scheme illustrating the scalable fabrication and self-integration of eight circle-shaped PG-PSSs connected in series (Figure 4a), with assistance of three shape-tailored customized masks for the formation of the first EG

layer (Figure 4b), second NGO layer (Figure 4c), and third EG layer (Figure 4d), respectively, on a single PET substrate.

The potential of perfect integration of PG-PSSs was demonstrated by operating 8 interconnected cells in series (Figure 4e,f). The CV curves with a nearly identical rectangular shape tested at 50 mV s^{-1} (Figure 4e), and GCD curves with a symmetric shape at current density of 20 μA cm^{-2} (Figure 4f) of the integrated PG-PSSs from 1 to 8 devices show a stepwise linear increase in the working voltage from 0.8 to 6.4 V with the number of cells and monotone decrease in the current and capacitance (Figure S25), indicative of excellent performance uniformity. It should be emphasized that this is an enormous advance of the one-pot construction of interconnected intelligent power source units, in which serial integrated devices are neither manually connected by metal (*e.g.*, copper tape)-based interconnects nor completely assembled on separated substrates.[8]

Except for the ability of fabricating serial interconnected cell packs, our arbitrary-shaped PG-PSSs could be readily interconnected, both in parallel and in series, to simultaneously change output capacitance and voltage that can meet the various requirements of integrated circuits. For instance, tandem PG-PSSs connected in a fashion of 2 parallel and 2 series from 1 to 4 devices (from 2, 4, 6, to 8 cells) disclosed not only the stepwise increase of voltage from 0.8 to 3.2 V but also almost double current output (Figure 4g) and discharge time (Figure 4h), while the operational voltage was invariable, compared to the interconnected PG-PSSs in series (from 1 to 4 cells) without parallel fashion under the same condition (Figures 4e,f and S26). Moreover, our power source-unitized PG-PSSs connected in 4 series (Figure 4f) and combined connection of 2 parallel and 4 series (Figure 4h) are able to readily power a light-emitting diode (LED). This result further highlights the great potential of our PG-PSSs as next-generation intelligent power source units for seamless integration into shape-confirmable electronics requiring variable operation voltage and capacitance.

CONCLUSIONS

In summary, we have demonstrated a versatile and scalable platform technology to create a class of PSSs on one substrate with exceptional shape conformability and advantageous features of superior flexibility, scalability, and integration as well as excellent compact charge storage, which are far beyond those achievable by conventional supercapacitor technologies. Both the efficient combination of printable technique and diversity of graphene materials simplify the fabrication of arbitrary-shaped PG-PSSs in both individual cell and modular power source units, with tailored voltage and capacitance, which overcomes the bottlenecks of traditional power source-related design and performance in electronics. Our strategy for PG-PSSs is highly reliable and scalable and compatible for various on-demand high-throughput printing techniques, in particular, high-resolution inkjet printing,[26] 3D printing,[27] and roll-to-roll process.[28] Through further improvement of the electrochemical performance, with a special focus on the combination of advanced materials such as high-capacitance electrode materials and high-voltage all-solid-state electrolytes,[63] our approach can be extended to other 2D materials for mass production of complex-shaped, fully printed PSSs with designable functionalities that are universally applicable to versatile-shaped flexible and wearable electronic devices.

METHODS

Fabrication of PG-PSSs. EG nanosheets were produced as described previously,[58] and the NGO solution was prepared by sonication of the supernatant of single-layer GO for 2 h using a high-shear mixer (BILON88-II, 200W), followed by filtration with a 220 nm cellulose membrane. To fabricate shape-tailored layer-structured films of EG/NGO/EG, corresponding shape-tailored customized masks were applied to modulate the shape patterns of PG-PSSs. To avoid short circuit, the masks for NGO patterns are a little wider (about hundreds to thousands of micrometers) than the masks for EG patterns. The distance between the air brush pistol and the substrate was kept at 2 cm, and the spray coating pressure of nitrogen gas was fixed at 0.1 MPa. The diameters of the air brush pistols for EG and NGO inks are 0.3 mm and 0.2 mm, respectively. Using these air brush pistols, with assistance of the first patterned mask, the EG ink with a concentration of 0.1 mg mL^{-1} was first spray-coated on a PET substrate to form the bottom EG film electrode and smoothly treated with the pressure of 3 MPa by tablet machine. Then, with the help of the second patterned mask, the middle NGO layer was covered on the EG film in the same way as the spray coating NGO solution (1.8 mg mL^{-1}) and followed by the treatment of 3 MPa. Afterward, the top layer of symmetric EG electrode with the same thickness was spray-coated on NGO layer using the third mask. Finally, the PG-PSSs were obtained.

For comparison, PG-CSSs with a stacked geometry were also fabricated sandwiching the H$_2$SO$_4$/PVA gel electrolyte between two EG film electrodes with the same film thickness on two individual PET substrates. Furthermore, using the same procedure as assembling the PG-PSSs, PG/HQ-PSSs were fabricated using two printable hybrid films of EG and HQ instead of the EG layers with HQ of 16 wt %, while other steps were kept the same. All of the parameters, *e.g.*, length and width, of different-shaped PG-PSSs were listed in Table S2.

Materials Characterizations. The characterizations of both the morphology and structure were performed by field emission SEM (JSM-7800F), HRTEM (JEM-2100), AFM (Veeco nanoscope multi-mode II-D), Raman spectrometer (LabRAM HR 800 Raman spectrometer, 532 nm), XRD (X'Pert Pro), XPS (Thermo ESCALAB 250Xi equipped with monochromatic Al Kα source of 1486.5 eV) and surface profiler (VEECO DEKTAK 150), standard four-point probe system (RTS-9).

Electrochemical Measurement. The electrochemical performance of the supercapacitors fabricated was evaluated by CV measurements carried out at different scan rates ranging from 1 mV s^{-1} to 500 mV s^{-1}, GCD profiles conducted at different current densities, and electrochemical impedance spectroscopy (EIS) recorded in the frequency range from 0.01 Hz to 100 kHz with a 5 mV ac amplitude, using an electrochemical workstation (CHI 760E).

ASSOCIATED CONTENT

Ⓢ Supporting Information

The Supporting Information is available free of charge on the ACS Publications website at DOI: 10.1021/acsnano.6b08435.

Experimental, materials characterization, electrochemical characterization, and additional figures, and a table used to performance comparison of our PG-PSSs with the state-of-the-art graphene-based interdigital planar supercapacitors (PDF)

AUTHOR INFORMATION

Corresponding Author

*E-mail: wuzs@dicp.ac.cn.

ORCID ⓘ

Zhong-Shuai Wu: 0000-0003-1851-4803
Xinhe Bao: 0000-0001-9404-6429

Author Contributions

Z.S.W., H.M.C., and X.H.B. proposed and supervised the overall project. S.H.Z. did the architecture design, fabrication, and electrochemical measurement of PG-PSSs. S.H.Z. and Z.S.W. analyzed the data. S.W. and C.L.S. participated in the preparation of electrolyte and the characterization of the related materials. X.Y.T. and Y.Z.T. prepared the NGO sheets. S.H.Z., Z.S.W., H.M.C., and X.H.B. co-wrote this paper.

Notes

The authors declare no competing financial interest.

REFERENCES

(1) Gates, B. D. Flexible Electronics. *Science* **2009**, *323*, 1566−1567.

(2) Rogers, J. A.; Someya, T.; Huang, Y. G. Materials and Mechanics for Stretchable Electronics. *Science* **2010**, *327*, 1603−1607.

(3) Gogotsi, Y. What Nano Can Do for Energy Storage. *ACS Nano* **2014**, *8*, 5369−5371.

(4) Choi, B. G.; Hong, J.; Hong, W. H.; Hammond, P. T.; Park, H. Facilitated Ion Transport in All-Solid-State Flexible Supercapacitors. *ACS Nano* **2011**, *5*, 7205−7213.

(5) Simon, P.; Gogotsi, Y. Materials for Electrochemical Capacitors. *Nat. Mater.* **2008**, *7*, 845−854.

(6) Yu, D. S.; Goh, K.; Wang, H.; Wei, L.; Jiang, W. C.; Zhang, Q.; Dai, L. M.; Chen, Y. Scalable Synthesis of Hierarchically Structured Carbon Nanotube-Graphene Fibres for Capacitive Energy Storage. *Nat. Nanotechnol.* **2014**, *9*, 555−562.

(7) Zhou, G.; Li, F.; Cheng, H.-M. Progress in Flexible Lithium Batteries and Future Prospects. *Energy Environ. Sci.* **2014**, *7*, 1307−1338.

(8) Wen, L.; Li, F.; Cheng, H.-M. Carbon Nanotubes and Graphene for Flexible Electrochemical Energy Storage: From Materials to Devices. *Adv. Mater.* **2016**, *28*, 4306−4337.

(9) Wu, Z.-S.; Liu, Z.; Parvez, K.; Feng, X.; Müllen, K. Ultrathin Printable Graphene Supercapacitors with AC Line-Filtering Performance. *Adv. Mater.* **2015**, *27*, 3669−3675.

(10) Kim, S. H.; Choi, K. H.; Cho, S. J.; Choi, S.; Park, S.; Lee, S. Y. Printable Solid-State Lithium-Ion Batteries: A New Route toward Shape-Conformable Power Sources with Aesthetic Versatility for Flexible Electronics. *Nano Lett.* **2015**, *15*, 5168−5177.

(11) Chen, X.; Lin, H.; Chen, P.; Guan, G.; Deng, J.; Peng, H. Smart, Stretchable Supercapacitors. *Adv. Mater.* **2014**, *26*, 4444−4449.

(12) Beidaghi, M.; Gogotsi, Y. Capacitive Energy Storage in Micro-Scale Devices: Recent Advances in Design and Fabrication of Micro-Supercapacitors. *Energy Environ. Sci.* **2014**, *7*, 867−884.

(13) Wang, S.; Zheng, S.; Wu, Z.-S.; Sun, C. Recent Advances in Graphene-Based Planar Micro-Supercapacitors. *Sci. Sin. Chim.* **2016**, *46*, 732−744.

(14) Lee, S. W.; Yabuuchi, N.; Gallant, B. M.; Chen, S.; Kim, B. S.; Hammond, P. T.; Shao-Horn, Y. High-Power Lithium Batteries from Functionalized Carbon-Nanotube Electrodes. *Nat. Nanotechnol.* **2010**, *5*, 531−537.

(15) Yang, X. W.; Cheng, C.; Wang, Y. F.; Qiu, L.; Li, D. Liquid-Mediated Dense Integration of Graphene Materials for Compact Capacitive Energy Storage. *Science* **2013**, *341*, 534−537.

(16) El-Kady, M. F.; Strong, V.; Dubin, S.; Kaner, R. B. Laser Scribing of High-Performance and Flexible Graphene-Based Electrochemical Capacitors. *Science* **2012**, *335*, 1326−1330.

(17) Chang, J.; Adhikari, S.; Lee, T. H.; Li, B.; Yao, F.; Pham, D. T.; Le, V. T.; Lee, Y. H. Leaf Vein-Inspired Nanochanneled Graphene Film for Highly Efficient Micro-Supercapacitors. *Adv. Energy Mater.* **2015**, *5*, 1500003.

(18) Yoon, Y.; Lee, K.; Kwon, S.; Seo, S.; Yoo, H.; Kim, S.; Shin, Y.; Park, Y.; Kim, D.; Choi, J.-Y.; Lee, H. Vertical Alignments of Graphene Sheets Spatially and Densely Piled for Fast Ion Diffusion in Compact Supercapacitors. *ACS Nano* **2014**, *8*, 4580−4590.

(19) Xu, Y.; Lin, Z.; Huang, X.; Liu, Y.; Huang, Y.; Duan, X. Flexible Solid-State Supercapacitors Based on Three-Dimensional Graphene Hydrogel Films. *ACS Nano* **2013**, *7*, 4042−4049.

(20) Lukatskaya, M. R.; Mashtalir, O.; Ren, C. E.; Dall'Agnese, Y.; Rozier, P.; Taberna, P. L.; Naguib, M.; Simon, P.; Barsoum, M. W.; Gogotsi, Y. Cation Intercalation and High Volumetric Capacitance of Two-Dimensional Titanium Carbide. *Science* **2013**, *341*, 1502−1505.

(21) Ghidiu, M.; Lukatskaya, M. R.; Zhao, M. Q.; Gogotsi, Y.; Barsoum, M. W. Conductive Two-Dimensional Titanium Carbide 'Clay' with High Volumetric Capacitance. *Nature* **2014**, *516*, 13970.

(22) Ling, Z.; Ren, C. E.; Zhao, M. Q.; Yang, J.; Giammarco, J. M.; Qiu, J. S.; Barsoum, M. W.; Gogotsi, Y. Flexible and Conductive MXene Films and Nanocomposites with High Capacitance. *Proc. Natl. Acad. Sci. U. S. A.* **2014**, *111*, 16676−16681.

(23) Kurra, N.; Ahmed, B.; Gogotsi, Y.; Alshareef, H. N. MXene-on-Paper Coplanar Microsupercapacitors. *Adv. Energy Mater.* **2016**, *6*, 1601372.

(24) Acerce, M.; Voiry, D.; Chhowalla, M. Metallic 1T Phase MoS₂ Nanosheets as Supercapacitor Electrode Materials. *Nat. Nanotechnol.* **2015**, *10*, 313−318.

(25) Kaempgen, M.; Chan, C. K.; Ma, J.; Cui, Y.; Gruner, G. Printable Thin Film Supercapacitors Using Single-Walled Carbon Nanotubes. *Nano Lett.* **2009**, *9*, 1872−1876.

(26) Choi, K.-H.; Yoo, J.; Lee, C. K.; Lee, S.-Y. All-Inkjet-Printed, Solid-State Flexible Supercapacitors on Paper. *Energy Environ. Sci.* **2016**, *9*, 2812−2821.

(27) Zhu, C.; Liu, T.; Qian, F.; Han, T. Y.-J.; Duoss, E. B.; Kuntz, J. D.; Spadaccini, C. M.; Worsley, M. A.; Li, Y. Supercapacitors Based on Three-Dimensional Hierarchical Graphene Aerogels with Periodic Macropores. *Nano Lett.* **2016**, *16*, 3448−3456.

(28) Bae, S.; Kim, H.; Lee, Y.; Xu, X. F.; Park, J. S.; Zheng, Y.; Balakrishnan, J.; Lei, T.; Kim, H. R.; Song, Y. I.; et al. Roll-To-Roll Production of 30-Inch Graphene Films for Transparent Electrodes. *Nat. Nanotechnol.* **2010**, *5*, 574−578.

(29) Kil, E.-H.; Choi, K.-H.; Ha, H.-J.; Xu, S.; Rogers, J. A.; Kim, M. R.; Lee, Y.-G.; Kim, K. M.; Cho, K. Y.; Lee, S.-Y. Imprintable, Bendable, and Shape-Conformable Polymer Electrolytes for Versatile-Shaped Lithium-Ion Batteries. *Adv. Mater.* **2013**, *25*, 1395−1400.

(30) Koo, M.; Park, K. I.; Lee, S. H.; Suh, M.; Jeon, D. Y.; Choi, J. W.; Kang, K.; Lee, K. J. Bendable Inorganic Thin-Film Battery for Fully Flexible Electronic Systems. *Nano Lett.* **2012**, *12*, 4810−4816.

(31) Jost, K.; Perez, C. R.; McDonough, J. K.; Presser, V.; Heon, M.; Dion, G.; Gogotsi, Y. Carbon Coated Textiles for Flexible Energy Storage. *Energy Environ. Sci.* **2011**, *4*, 5060−5067.

(32) Li, N.; Chen, Z. P.; Ren, W. C.; Li, F.; Cheng, H. M. Flexible Graphene-Based Lithium Ion Batteries with Ultrafast Charge and Discharge Rates. *Proc. Natl. Acad. Sci. U. S. A.* **2012**, *109*, 17360−17365.

(33) Chen, W.; Rakhi, R. B.; Hu, L. B.; Xie, X.; Cui, Y.; Alshareef, H. N. High-Performance Nanostructured Supercapacitors on A Sponge. *Nano Lett.* **2011**, *11*, 5165−5172.

(34) Lang, X. Y.; Hirata, A.; Fujita, T.; Chen, M. W. Nanoporous Metal/Oxide Hybrid Electrodes for Electrochemical Supercapacitors. *Nat. Nanotechnol.* **2011**, *6*, 232−236.

(35) Liu, Z.; Wu, Z.-S.; Yang, S.; Dong, R.; Feng, X.; Müllen, K. Ultraflexible In-Plane Micro-Supercapacitors by Direct Printing of Solution-Processable Electrochemically Exfoliated Graphene. *Adv. Mater.* **2016**, *28*, 2217−2222.

(36) Hu, L. B.; Choi, J. W.; Yang, Y.; Jeong, S.; La Mantia, F.; Cui, L. F.; Cui, Y. Highly Conductive Paper for Energy-Storage Devices. *Proc. Natl. Acad. Sci. U. S. A.* **2009**, *106*, 21490−21494.

(37) Hu, L. B.; Pasta, M.; La Mantia, F.; Cui, L. F.; Jeong, S.; Deshazer, H. D.; Choi, J. W.; Han, S. M.; Cui, Y. Stretchable, Porous, and Conductive Energy Textiles. *Nano Lett.* **2010**, *10*, 708−714.

(38) Ma, Y.; Li, P.; Sedloff, J. W.; Zhang, X.; Zhang, H.; Liu, J. Conductive Graphene Fibers for Wire-Shaped Supercapacitors Strengthened by Unfunctionalized Few-Walled Carbon Nanotubes. *ACS Nano* **2015**, *9*, 1352−1359.

(39) Kou, L.; Huang, T. Q.; Zheng, B. N.; Han, Y.; Zhao, X. L.; Gopalsamy, K.; Sun, H. Y.; Gao, C. Coaxial Wet-Spun Yarn Supercapacitors for High-Energy Density and Safe Wearable Electronics. *Nat. Commun.* **2014**, *5*, 3754.

(40) Yu, D. S.; Qian, Q. H.; Wei, L.; Jiang, W. C.; Goh, K. L.; Wei, J.; Zhang, J.; Chen, Y. Emergence of Fiber Supercapacitors. *Chem. Soc. Rev.* **2015**, *44*, 647−662.

(41) Liu, L. L.; Niu, Z. Q.; Zhang, L.; Zhou, W. Y.; Chen, X. D.; Xie, S. S. Nanostructured Graphene Composite Papers for Highly Flexible and Foldable Supercapacitors. *Adv. Mater.* **2014**, *26*, 4855−4862.

(42) Xu, S.; Zhang, Y. H.; Cho, J.; Lee, J.; Huang, X.; Jia, L.; Fan, J. A.; Su, Y. W.; Su, J.; Zhang, H. G.; et al. Stretchable Batteries with Self-Similar Serpentine Interconnects and Integrated Wireless Recharging Systems. *Nat. Commun.* **2013**, *4*, 1543.

(43) Chen, T.; Xue, Y.; Roy, A. K.; Dai, L. Transparent and Stretchable High-Performance Supercapacitors Based on Wrinkled Graphene Electrodes. *ACS Nano* **2014**, *8*, 1039−1046.

(44) Yoo, J. J.; Balakrishnan, K.; Huang, J.; Meunier, V.; Sumpter, B. G.; Srivastava, A.; Conway, M.; Reddy, A. L. M.; Yu, J.; Vajtai, R.; Ajayan, P. M. Ultrathin Planar Graphene Supercapacitors. *Nano Lett.* **2011**, *11*, 1423−1427.

(45) Wu, Z.-S.; Feng, X.; Cheng, H.-M. Recent Advances in Graphene-Based Planar Micro-Supercapacitors for On-Chip Energy Storage. *Natl. Sci. Rev.* **2014**, *1*, 277−292.

(46) Liu, J. Charging Graphene for Energy. *Nat. Nanotechnol.* **2014**, *9*, 739−741.

(47) Meng, C.; Maeng, J.; John, S. W. M.; Irazoqui, P. P. Ultrasmall Integrated 3D Micro-Supercapacitors Solve Energy Storage for Miniature Devices. *Adv. Energy Mater.* **2014**, *4*, 1301269.

(48) Wang, K.; Zou, W. J.; Quan, B. G.; Yu, A. F.; Wu, H. P.; Jiang, P.; Wei, Z. X. An All-Solid-State Flexible Micro-Supercapacitor on A Chip. *Adv. Energy Mater.* **2011**, *1*, 1068−1072.

(49) Lin, J.; Zhang, C. G.; Yan, Z.; Zhu, Y.; Peng, Z. W.; Hauge, R. H.; Natelson, D.; Tour, J. M. 3-Dimensional Graphene Carbon Nanotube Carpet-Based Microsupercapacitors with High Electrochemical Performance. *Nano Lett.* **2013**, *13*, 72−78.

(50) Yoo, J. J.; Balakrishnan, K.; Huang, J. S.; Meunier, V.; Sumpter, B. G.; Srivastava, A.; Conway, M.; Reddy, A. L. M.; Yu, J.; Vajtai, R.; Ajayan, P. M. Ultrathin Planar Graphene Supercapacitors. *Nano Lett.* **2011**, *11*, 1423−1427.

(51) Gao, W.; Singh, N.; Song, L.; Liu, Z.; Reddy, A. L. M.; Ci, L. J.; Vajtai, R.; Zhang, Q.; Wei, B. Q.; Ajayan, P. M. Direct Laser Writing of Micro-Supercapacitors on Hydrated Graphite Oxide Films. *Nat. Nanotechnol.* **2011**, *6*, 496−500.

(52) El-Kady, M. F.; Kaner, R. B. Scalable Fabrication of High-Power Graphene Micro-Supercapacitors for Flexible and On-Chip Energy Storage. *Nat. Commun.* **2013**, *4*, 1475.

(53) Wu, Z.-S.; Parvez, K.; Feng, X. L.; Müllen, K. Graphene-Based In-Plane Micro-Supercapacitors with High Power and Energy Densities. *Nat. Commun.* **2013**, *4*, 2487.

(54) Lu, X. H.; Yu, M. H.; Zhai, T.; Wang, G. M.; Xie, S. L.; Liu, T. Y.; Liang, C. L.; Tong, Y. X.; Li, Y. High Energy Density Asymmetric Quasi-Solid-State Supercapacitor Based on Porous Vanadium Nitride Nanowire Anode. *Nano Lett.* **2013**, *13*, 2628−2633.

(55) Huang, L.; Chen, D. C.; Ding, Y.; Feng, S.; Wang, Z. L.; Liu, M. L. Nickel-Cobalt Hydroxide Nanosheets Coated on $NiCo_2O_4$ Nanowires Grown on Carbon Fiber Paper for High-Performance Pseudocapacitors. *Nano Lett.* **2013**, *13*, 3135−3139.

(56) Yuan, L.; Lu, X.-H.; Xiao, X.; Zhai, T.; Dai, J.; Zhang, F.; Hu, B.; Wang, X.; Gong, L.; Chen, J.; et al. Flexible Solid-State Supercapacitors Based on Carbon Nanoparticles/MnO_2 Nanorods Hybrid Structure. *ACS Nano* **2012**, *6*, 656−661.

(57) Zhang, C.; Yin, H.; Han, M.; Dai, Z.; Pang, H.; Zheng, Y.; Lan, Y.-Q.; Bao, J.; Zhu, J. Two-Dimensional Tin Selenide Nanostructures for Flexible All-Solid-State Supercapacitors. *ACS Nano* **2014**, *8*, 3761−3770.

(58) Parvez, K.; Li, R. J.; Puniredd, S. R.; Hernandez, Y.; Hinkel, F.; Wang, S. H.; Feng, X. L.; Müllen, K. Electrochemically Exfoliated Graphene As Solution-Processable, Highly Conductive Electrodes for Organic Electronics. *ACS Nano* **2013**, *7*, 3598−3606.

(59) Zhang, Q.; Scrafford, K.; Li, M. T.; Cao, Z. Y.; Xia, Z. H.; Ajayan, P. M.; Wei, B. Q. Anomalous Capacitive Behaviors of Graphene Oxide Based Solid-State Supercapacitors. *Nano Lett.* **2014**, *14*, 1938−1943.

(60) Pech, D.; Brunet, M.; Durou, H.; Huang, P. H.; Mochalin, V.; Gogotsi, Y.; Taberna, P. L.; Simon, P. Ultrahigh-Power Micrometre-Sized Supercapacitors Based on Onion-Like Carbon. *Nat. Nanotechnol.* **2010**, *5*, 651−654.

(61) Roldan, S.; Blanco, C.; Granda, M.; Menendez, R.; Santamaria, R. Towards A Further Generation of High-Energy Carbon-Based Capacitors by Using Redox-Active Electrolytes. *Angew. Chem., Int. Ed.* **2011**, *50*, 1699−1701.

(62) Shao, Y.; El-Kady, M. F.; Wang, L. J.; Zhang, Q.; Li, Y.; Wang, H.; Mousavi, M. F.; Kaner, R. B. Graphene-Based Materials for Flexible Supercapacitors. *Chem. Soc. Rev.* **2015**, *44*, 3639−3665.

(63) Simon, P.; Gogotsi, Y. Capacitive Energy Storage in Nano-structured Carbon-Electrolyte Systems. *Acc. Chem. Res.* **2013**, *46*, 1094−1103.